

# Calculation of a Reaction Path for KOH Catalyzed Ring-Opening Polymerization of Hexamethylcyclotrisiloxane

J. D. Kress,<sup>\*,†</sup> P. C. Leung,<sup>\*,#</sup> G. J. Tawa,<sup>†,§</sup> and P. J. Hay<sup>†</sup>

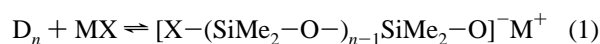
Contribution from the Theoretical Division, Los Alamos National Laboratory, Los Alamos, New Mexico 87545, and Technical Computing Department, 3M Corporation, St. Paul, Minnesota 55144-1000

Received April 11, 1996. Revised Manuscript Received December 23, 1996<sup>⊗</sup>

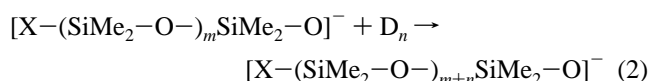
**Abstract:** Polysiloxanes represent an important class of industrial polymers. Traditionally, poly(dimethylsiloxane) (PDMS) can be prepared by base-catalyzed ring-opening of cyclic dimethylsiloxanes. *Ab initio* electronic calculations were conducted to examine a reaction path for the KOH catalyzed ring-opening polymerization of hexamethylcyclotrisiloxane (D<sub>3</sub>). The overall picture that emerges is initial side-on attack by KOH on a Si–O bond in the D<sub>3</sub> ring leading to a stable addition complex with a 5-fold coordinated Si atom. The reaction path leads to a five-coordinate transition state, then to a stable insertion product (KOH inserts into the ring). The relative stability of a ring-opened product HO[Si(CH<sub>3</sub>)<sub>2</sub>O]<sub>3</sub>K is also considered. The energy along the reaction path was modeled both in the gas phase and in a moderately polar solvent (tetrahydrofuran, THF). The solvation energy was calculated using a recent implementation of an electrostatic model, where the solute molecule is placed in a non-spherical cavity in a dielectric continuum. The effect of basis set and electron correlation on the gas-phase energy and the effect of basis set on the solvation energy was studied. Along the solvated reaction path calculated at the Hartree–Fock level (with a 6-31G\* basis set for the Si and O atoms), the apparent transition state energy is nearly equal to the reactants energy and is 4 kcal/mol above the addition complex energy.

## Introduction

The importance of poly(dialkylsiloxane)s as inorganic backbone polymers is well established.<sup>1,2</sup> The synthesis of linear siloxane polymers can be divided into two general classes;<sup>3</sup> polycondensation of bifunctional siloxanes and ring-opening polymerization of cyclic oligosiloxanes. The mechanism of the latter initiated (catalyzed) by a base (anionic polymerization) is the focus of this work. A shorthand notation is useful for referring to the cyclic siloxanes. The (CH<sub>3</sub>)<sub>2</sub>SiO unit will be represented as D, *i.e.* the cyclic trimer hexamethylcyclotrisiloxane is denoted as D<sub>3</sub>. The base-catalyzed reaction involves a catalyst MX, where M is an alkali metal or ammonium cation and X is a counterion. The siloxane ring-opening polymerization process of interest is composed of an initiation reaction



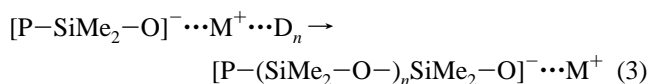
followed by a chain propagation step,



where  $[X-(SiMe_2-O-)_{m-1}SiMe_2-O]^-$  is the growing species (denoted P later) and Me is a methyl (CH<sub>3</sub>) group. For  $n > 3$ ,

(1) is represented as reversible and the polymerization is controlled by thermodynamics.<sup>1,2</sup> But for  $n = 3$  the reversibility is greatly suppressed due to ring strain in D<sub>3</sub> (absent for rings with  $n > 3$ ) and the polymerization is controlled by kinetics.<sup>1,2</sup>

According to one proposed mechanism,<sup>3,4</sup> a cation (*e.g.* K<sup>+</sup> or Li<sup>+</sup>) forms a complex with the growing species and D<sub>n</sub>. Rearrangement of the complexes occurs, resulting in extension of the siloxane polymer chain by the reaction



A multidentate structure between the cation and the O atoms in the D<sub>n</sub> ring has been proposed<sup>4</sup> as the transition state in order to explain the trend in the rate of reaction for  $n = 5$  to 9. The multidentate structure is akin to the interaction of a cation with polydentate ether ligands in crown ethers. Other studies, however, suggest a mechanism in which the anion attacks D<sub>n</sub> directly (eq 2) and the metal ion is not involved in the ring-opening step.<sup>5,1,2</sup> For the anion mechanism, a pentavalent (5-fold coordinated) Si atom intermediate was proposed.<sup>5</sup> Structural entropy changes in various conformations of ligand attachment to trigonal bipyramidal structures were used to explain the observed trend in reactivity for D<sub>6</sub> and D<sub>7</sub>. The level of association between the cation and the growing species depends on the polarity of the solvent used in the process.

Disiloxane, (SiH<sub>3</sub>)O(SiH<sub>3</sub>), has been the subject of many electronic structure calculations.<sup>6–9</sup> The Si–O–Si bond angle in disiloxane is very flexible and thus the geometry is a challenge

(4) Mazurek, M.; Chojnowski, J. *Makromol. Chem.* **1977**, *178*, 1005.

(5) Laita, Z.; Jelinek, M. *Vysokomol. Soed.* **1962**, *4*, 1739. [*Polym. Sci. USSR (Engl. Transl.)* **1965**, *4*, 535.]

(6) Grigoras, S.; Lane, T. H. *J. Comput. Chem.* **1987**, *8*, 84.

(7) Shambayati, S.; Blake, J. F.; Wierschke, S. G.; Jorgensen, W. L.; Schreiber, S. L. *J. Am. Chem. Soc.* **1990**, *112*, 697.

(8) Luke, B. T. *J. Phys. Chem.* **1993**, *97*, 7505.

(9) Koput, J. *J. Phys. Chem.* **1995**, *99*, 15874. Nicholas, J. B.; Feyereisen, M. J. *Chem. Phys.* **1995**, *103*, 8031. Csonka, G. I.; Reffy, J. *THEOCHEM.* **1995**, *332*, 187. Baer, M. R.; Sauer, J. *Chem. Phys. Lett.* **1994**, *226*, 405.

<sup>†</sup> Los Alamos National Laboratory.

<sup>‡</sup> 3M Corporation.

<sup>#</sup> Deceased.

<sup>§</sup> Present address: NCI-Frederick Cancer Research and Development Center, Frederick, MD 21702-1201.

<sup>⊗</sup> Abstract published in *Advance ACS Abstracts*, February 1, 1997.

(1) Saam, J. C. In *Silicon-Based Polymer Science: A Comprehensive Resource*; Ziegler, J. M., Gordon Fearon, F. W., Eds.; American Chemical Society: Washington, DC, 1990; pp 71–90.

(2) Wright, P. V. In *Ring Opening Polymerization*; Ivin, K. J., Saegusa, T., Eds.; Elsevier: New York, 1984; pp 1055–1133.

(3) Chojnowski, J. In *Siloxane Polymers*; Clarson, S. J., Semylen, J. A., Eds.; Prentice Hall: Englewood Cliffs, NJ, 1993; pp 1–71. Chojnowski, J. In *Silicon Chemistry*; Corey, J. Y., Corey, E. R., Gaspar, P. P., Eds.; Ellis Horwood: New York, 1988; pp 297–306.

**Table 1.** Geometries for the D<sub>3</sub> Ring

Si <sub>3</sub> O basis set	C,H basis set	Si–O bond distance (Å)	Si–O–Si bond angle (deg)	O–Si–O bond angle (deg)
3-21G	STO-3G	1.672	137.1	102.9
3-21G(d)	STO-3G	1.642	133.1	106.9
6-31G*	STO-3G	1.652	134.1	106.9
6-31G*	3-21G	1.647	134.0	106.0
(6-31+G*) <sup>a</sup>	3-21G	1.647	134.3	105.7
3-21G(2d)	STO-3G	1.635	132.6	107.4
exptl (ref 15)		1.635 ± 0.002	131.6 ± 0.4	107.8 ± 0.7

<sup>a</sup> The diffuse function is added only to the O atoms.

to predict correctly. Molecular mechanics force fields based on *ab initio* calculations on disiloxane and other small molecules have been used to study<sup>10</sup> the torsional barrier in hexamethyl-disiloxane and structural conformations of D<sub>4</sub>. *Ab initio* calculations on several conformation of polysiloxane, (H<sub>2</sub>SiO)<sub>n</sub> for n = 3, 4, and 5, have also been reported.<sup>11</sup> Calculations on small siloxane molecules have also been used as models for zeolites.<sup>12</sup>

The present work focuses on the kinetically controlled reaction KOH + D<sub>3</sub> → HO[Si(CH<sub>3</sub>)<sub>2</sub>O]<sub>3</sub>K. For this reaction, KOH acts as the catalyst. The energy along the reaction path was modeled both in the gas phase and in a moderately polar solvent (tetrahydrofuran, THF). The solvation energy was calculated using a recent implementation of an electrostatic model, where the solute molecule is placed in a non-spherical cavity in a dielectric continuum.

## Computational Method

**Electronic Structure.** Calculations were performed using the GAUSSIAN 92 and GAUSSIAN 94 programs.<sup>13</sup> The choice of basis sets resulted from a balance between quantitative accuracy and computational effort. To this end a modest STO-3G basis was used throughout for carbon and hydrogen atoms (unless specified otherwise) and the LANL2DZ effective core potential<sup>14</sup> (ECP) was used throughout for potassium (unless specified otherwise). For silicon and oxygen atoms, 3-21G, 3-21G(d), 6-31G\*, and 3-21G(2d) bases were examined. For the 3-21G(d) and 6-31G\* bases, polarization exponents of α<sub>d</sub> = 0.45 and 0.8 were used<sup>13</sup> for Si and O, respectively. In studies of organosilicon compounds, a range of α<sub>d</sub> values for Si have been used (see ref 6 for a summary); for example, Gordon<sup>15</sup> determined α<sub>d</sub> = 0.395 based on optimizing α<sub>d</sub> with respect to the energy of SiH<sub>4</sub>. For the 3-21G(2d) basis, the two polarization exponents were assigned as α<sub>d</sub><sup>+</sup> = 2 α<sub>d</sub> and α<sub>d</sub><sup>-</sup> = α<sub>d</sub>/2. The effect of basis set on the conformation for D<sub>3</sub> has been studied (Table 1). Nicholas et al.<sup>16</sup> find that a double polarization basis is needed to obtain a reasonable nonlinear Si–O–Si angle, α(Si–O–Si), for disiloxane, which is very flexible and is thus difficult to converge. It has been suggested<sup>7–9,16</sup> that even larger bases and/or correlated wave functions may be necessary to accurately predict the precise geometry of disiloxane, although this level of accuracy is beyond the scope of the present studies. The 3-21G basis results in a Si–O bond distance, r(Si–O), that is about 0.04 Å too long, α(Si–O–Si) that is about 6° too large, and a O–Si–O angle, α(O–Si–O), that is 5° too small, compared to experiment.<sup>17</sup> The 6-31G\* basis results in r(Si–O) that is about 0.02 Å too long, α(Si–O–Si) that is 2° too large, and α(O–Si–O) that is 2° too small. The 3-21G(2d) basis results in r(Si–O) that agrees with experiment, α(Si–

O–Si) that is 1° too large, and α(O–Si–O) that is less than 1° too small. Kudo *et al.* calculated<sup>11</sup> the structure for the equivalent D<sub>3</sub> cyclosiloxane (H<sub>2</sub>SiO)<sub>3</sub> ring. For the 6-31G\* basis set on all atoms, they find r(Si–O) = 1.646 Å, α(Si–O–Si) = 133.2°, and α(O–Si–O) = 106.8° in good agreement with the present 6-31G\* results for PDMS. Both the 3-21G and 6-31G\* bases were used in the reaction path studies described later. Although more accurate, the use of the 3-21G(2d) basis to determine the reaction path is too computationally expensive.

The effect of basis set for the C and H atoms on the conformation of D<sub>3</sub> was tested by comparing the STO-3G results with the more accurate 3-21G results while using the same basis set (6-31G\*) for Si and O (Table 1). r(Si–O) changes by less than 0.01 Å, α(Si–O–Si) changes by 0.2°, and α(O–Si–O) changes by 0.1°. These changes are relatively small, therefore the STO-3G basis set for C and H atoms was deemed sufficient for the reaction path studies described later.

The optimized geometries were determined by analytic gradient techniques. The use of solely **Z**-matrix coordinates (bond distances, bond and dihedral angles) for optimizing ring structures using GAUSSIAN 92 leads to difficulty as the ring tends to pop open every few optimization steps. Instead, a mixed-coordinate system based on Cartesian coordinates for the ring atoms (Si and O) and for the KOH molecule was successfully combined with a **Z**-matrix representation for the CH<sub>3</sub> side groups. Optimizations of ring-containing molecules were also checked using redundant internal coordinates<sup>18</sup> in GAUSSIAN 94.

**Solvation Model.** First, the quantum mechanical electrostatic potential is calculated on a grid surrounding the solute molecule for each optimized geometry along the gas-phase reaction path. Then an electrostatic potential (ESP) fit<sup>19</sup> is performed to obtain a set of atom-centered charges. Next a molecular volume is constructed around the solute molecule; it is composed of a union of spheres centered at each atom of the solute. Each sphere has a radius about equal to the van der Waals radius of the atom upon which it is centered. The following cavity radii were used:<sup>20</sup> R(K) = 2.172 Å, R(O) = 1.65 Å, R(Si) = 2.0 Å, R(C) = 1.85 Å, R(H) = 1.0 Å. It is assumed that the solvent resides outside the molecular surface, and is a dielectric continuum characterized by a static dielectric constant, ε. To represent tetrahydrofuran (THF), a moderately polar solvent was used in polymerization, ε = 8.2 (ref 21). The region inside of the molecular surface is assigned ε = 1. The set of atom charges determined from the electronic structure calculation is then used in the governing macroscopic Poisson equation which is solved<sup>22</sup> to obtain the response of the solvent to the solute charge density. This response is in the form of a set of polarization charges residing on the solute molecular surface. With the polarization charges in hand the classical electrostatic solvation energy is given by the Coulomb interaction between the polarization charges representing the solvent with the atom-centered charges of the solute:

$$\Delta G(\text{solv}) = \frac{1}{2} \sum_A \left[ \sum_S \left[ \frac{Q(A)q(S)}{|\vec{R}(A) - \vec{R}(S)|} \right] \right] \quad (4)$$

Here the double sum runs over atom charges and polarization charges,

(18) Pulay, P.; Fogarisi, G.; Pang, F.; Boggs, J. E. *J. Am. Chem. Soc.* **1979**, *101*, 2550. Fogarisi, G.; Zhou, X.; Taylor, P.; Pulay, P. *J. Am. Chem. Soc.* **1992**, *114*, 8191.

(19) Breneman, C. M.; Wiberg, K. B. *J. Comput. Chem.* **1990**, *11*, 361.

(20) For K atoms: Rashin, A. A.; Honig, B. *J. Phys. Chem.* **1985**, *89*, 5588. For O, C, H, and Si atoms: Weiner, S. J.; Kollman, P. A.; Case, D. A.; Singh, U. C.; Ghio, C.; Alagona, G.; Profeta, S., Jr.; Weiner, P. *J. J. Am. Chem. Soc.* **1984**, *106*, 765 (Table 19).

(21) Holland, R. S.; Smyth, C. P. *J. Phys. Chem.* **1955**, *59*, 1088.

(22) Tawa, G. J.; Pratt, L. R. In *Structure and reactivity in aqueous solution: Characterization of chemical and biological systems*; Cramer, C. J., Truhlar, D. G., Eds.; ACS Symp. Ser. 568; American Chemical Society: Washington, DC, 1984; p 60. Tawa, G. J.; Pratt, L. R. *J. Am. Chem. Soc.* **1995**, *117*, 1625. Corcelli, S. A.; Kress, J. D.; Pratt, L. R.; Tawa, G. J. *BIOCOMPUTING. Proceedings of the 1996 Pacific Symposium*; Hunter, L., Klein, T. E., Eds.; World Scientific: Singapore, 1995; pp 142–159. Pratt, L. R.; Tawa, G. J.; Hummer, G.; Garcia, A. E.; Corcelli, S. A. Boundary Integral Methods for the Solution of the Poisson Equation of Continuum Solvation Models. *Int. J. Quantum Chem.* In press. Tawa, G. J.; Martin, R. L.; Pratt, L. R.; Russo, T. V. *J. Phys. Chem.* **1996**, *100*, 1515.

(10) Grigoras, S.; Lane, T. H. *J. Comput. Chem.* **1988**, *9*, 25.

(11) Kudo, T.; Hashimoto, F.; Gordon, M. S. *J. Comput. Chem.* **1996**, *17*, 1163.

(12) Sauer, J. *Chem. Rev.* **1989**, *89*, 199.

(13) Frisch, M. *et al.* GAUSSIAN 92, Revision A; Gaussian Inc.: Pittsburgh, PA, 1992. Frisch, M. *et al.* GAUSSIAN 94, Revision D.3; Gaussian Inc.: Pittsburgh, PA, 1995.

(14) Hay, P. J.; Wadt, W. R. *J. Chem. Phys.* **1985**, *82*, 299.

(15) Gordon, M. *Chem. Phys. Lett.* **1980**, *76*, 163.

(16) Nicholas, J. B.; Winans, R. E.; Harrison, R. J.; Iton, L. E.; Curtiss, L. A.; Hopfinger, A. J. *J. Phys. Chem.* **1992**, *96*, 10247.

(17) Oberhammer, H.; Zeil, W.; Fogarisi, G. *J. Mol. Struct.* **1973**, *18*, 309.

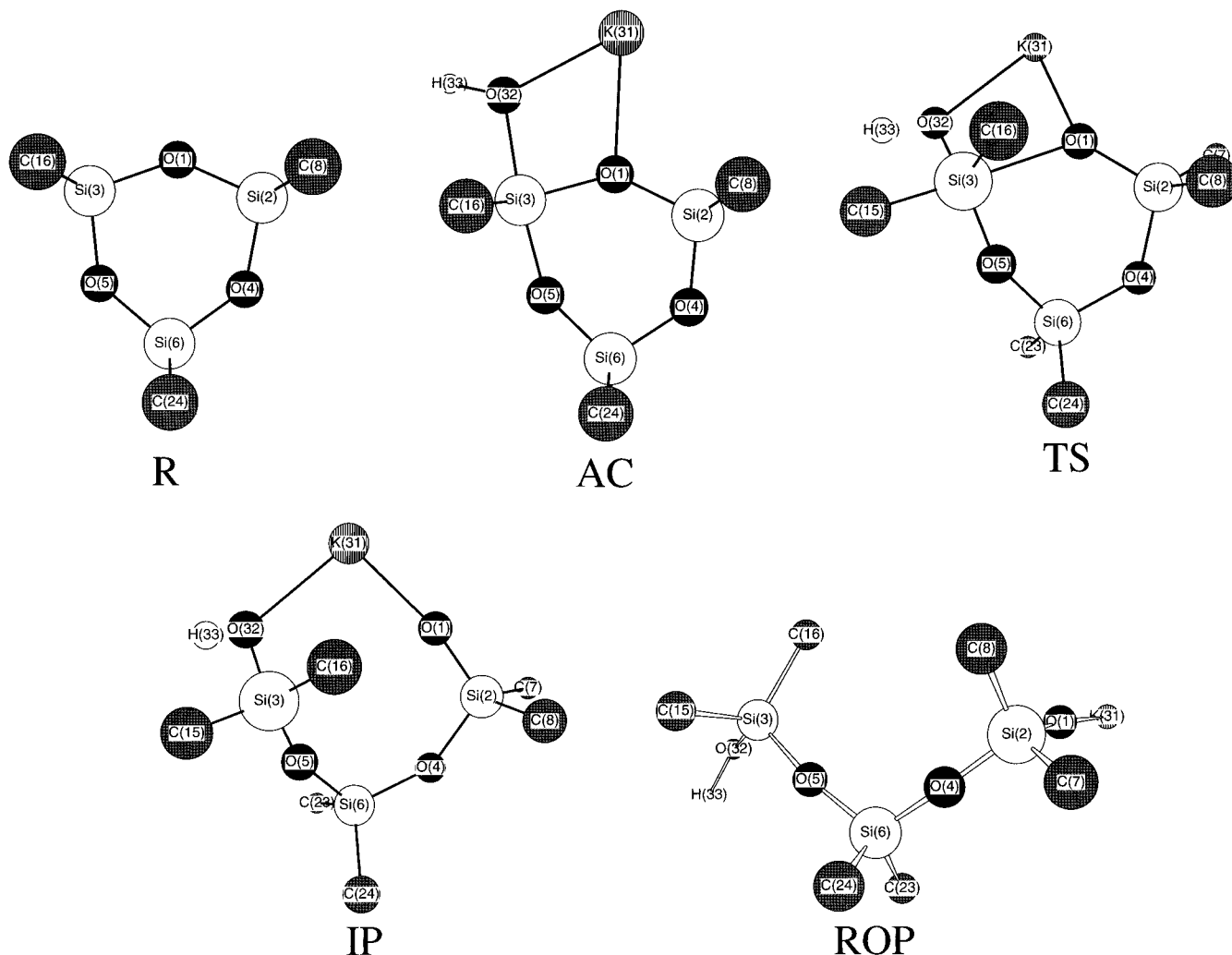


**Figure 1.** Structures of critical points along the reaction path for KOH catalyzed ring-opening polymerization of  $D_3$ : (R) reactant (isolated KOH not shown); (AC) addition complex; (TS) transition state; (IP) insertion product; (ROP) Ring-opened product. H atoms on methyl groups are omitted for clarity. C atoms behind the plane of the paper are hidden by out-of-plane C atoms in R and AC.

$Q(A)$  is the charge of atom A located at  $\vec{R}(A)$  determined from the ESP fit, and  $q(S)$  is the polarization charge at surface point  $\vec{R}(S)$  determined by solving Poisson's equation.<sup>22</sup> Finally, the potential of mean force is given by  $W = E(\text{electronic}) + \Delta G(\text{solv})$ . All results presented later utilize 256 surface elements for solving Poisson's equation.

## Results

A reaction path for the KOH catalyzed ring-opening of  $D_3$  in the gas phase was constructed. The calculated 3-21G structures of critical points along the reaction path are shown in Figure 1 and the structures of two metastable adducts are shown in Figure 2. (The atoms are numbered for reference in Figures 1 and 2). The 3-21G and 6-31G\* gas-phase energies along the reaction path are shown in Figure 3. The specific structures along the reaction path are discussed in the next section. For  $r > 0$  ( $r = 0$  is the addition complex structure, AC), the reaction coordinate  $r$  is the Si(3)–O(1) bond distance. For  $r < 0$ ,  $r$  is not specific, but is only representative of going downhill in energy from R (reactant) to AC. In Table 2, representative geometries, charges, and energies for 6-31G\* structures along the reaction path are given. Solvation energies along the reaction coordinate were obtained by calculating the potential of mean force using the dielectric continuum model<sup>22</sup> described above. In Tables 3 and 4, a summary of the relative energies for critical points along the gas-phase and solvated reaction path, respectively, is given. The basis set used to optimize the geometry and to calculate the energy is specified.

In all cases, the HF method was used to optimize the geometry. The effect of electron correlation on the energy was calculated with Møller–Plesset 2nd-order perturbation theory (MP2) at the HF geometry. In Figure 4, the HF/3-21G gas-phase reaction path energy and the corresponding potential of mean force calculated is plotted. Figure 4 explicitly shows the number of points calculated to define the reaction path from the addition complex to the insertion product. A comparison between the 6-31G\* gas-phase energy and potentials of mean force (solvated energy) along the reaction path is shown in Figure 5.

## Discussion

**Gas-Phase Calculations.** Starting at the left-most point in Figure 3, consider the reactants, KOH and a  $D_3$  molecule at infinite separation. The calculated and experimental<sup>17</sup> conformation for  $D_3$  is planar as shown in Figure 1 (structure R).  $D_3$  is strained, whereas the higher  $D_n$  ( $n > 3$ ) rings are not.<sup>1–3</sup> The relative ring strain in  $D_3$  was estimated to be 11 kcal/mol by calculating the difference in the 3-21G\* energy of the reaction



for  $n = 3$  and 4.

The initial step along the reaction path starting from the reactants is the formation of a KOH/ $D_3$  adduct. The optimization was constrained by fixing the planar  $D_3$  at the STO-3G geometry and only allowing the KOH to coordinate side-on to

**Table 2.** Representative Geometries, Charges, and Energies for Various KOH-D<sub>3</sub> Structures<sup>a</sup>

quantity	structures				
	R	AC	TS	IP	ROP
bond distance (Å)					
Si(3)–O(1) <sup>b</sup>	1.656 <sup>c</sup>	1.743	1.943	3.754	5.643
K(31)–O(1)	na <sup>d</sup>	2.441	2.516	2.380	2.351
K(31)–O(32)	2.270	2.423	2.501	2.682	6.228
Si(3)–O(32)	na	1.934	1.765	1.707	1.676
Si(3)–O(5)	1.647 <sup>c</sup>	1.785	1.696	1.616	1.630
angle (deg)					
O(1)–Si(3)–O(5)		91.10	86.84		
O(1)–Si(3)–O(32)		83.05	81.53		
O(5)–Si(3)–O(32)		174.15	121.68		
O(1)–Si(3)–C(15)		118.77	171.90		
O(1)–Si(3)–C(16)		118.91	87.76		
C(15)–Si(3)–C(16)		121.61	99.49		
charge (CHELPG)					
O(1)	–0.87	–0.77	–0.92	–1.18	–1.17
Si(3)	1.24	1.13	1.28	1.17	1.09
O(5)	–0.87	–0.92	–0.88	–0.79	–0.80
K(31)	0.94	0.93	0.93	0.94	0.94
O(32)	–1.34	–1.13	–0.96	–0.93	–0.87
energy <sup>e</sup> (hartree)	–0.94594	–0.97412	–0.96938	–0.98913	–0.96889

<sup>a</sup> 6-31G\* basis set used for Si and O. For K, the LANL2DZ ECP was used, and for C and H, the STO-3G basis set was used. <sup>b</sup> Reaction coordinate. <sup>c</sup> This calculation yielded alternating Si–O bond lengths. <sup>d</sup> Not applicable. <sup>e</sup> Total electronic energy relative to –1429 hartrees.

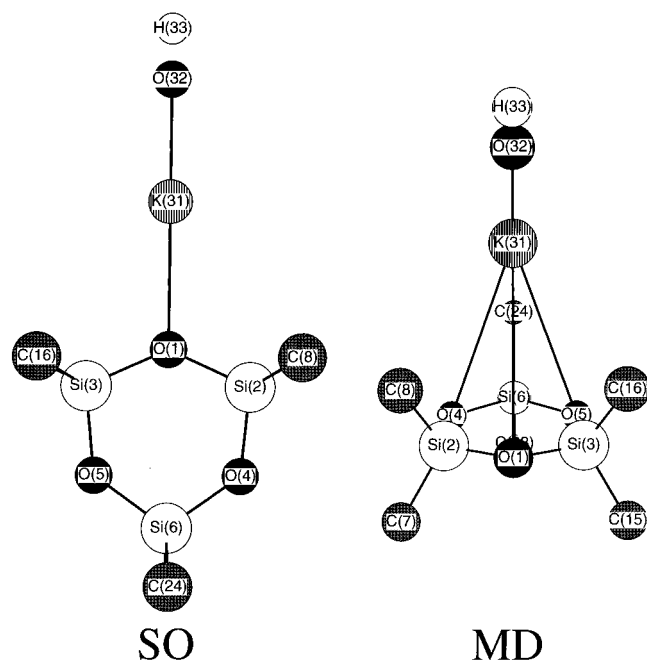


**Figure 2.** Structures of metastable adducts of KOH and D<sub>3</sub>: (SO) side-on adduct; (MD) multidentate adduct. H atoms on methyl groups are omitted for clarity. C atoms behind the plane of the paper are hidden by out-of-plane C atoms in SO.

an O atom in the ring. This is shown in Figure 2 (side-on structure, SO). This side-on adduct energy is about 11 kcal/mol below the 3-21G reactants energy. A multidentate interaction between the K atom and the O atoms in the D<sub>n</sub> ring has been proposed<sup>4</sup> as the transition state for this reaction in general. This structure (Figure 2, multidentate structure, MD) is akin to the interaction of a cation with polydentate ether ligands in crown ethers. The multidentate adduct energy, calculated in the same manner as the side-on adduct energy, is about 2 kcal/mol below the reactants energy and thus about 9 kcal/mol above the side-on adduct energy. The multidentate adduct is less stable than the side-on adduct for D<sub>3</sub> due to steric hindrance of the methyl groups on the Si atoms which shield the K interacting with the O atoms in the ring. This is not true<sup>23</sup> for larger (*n* > 3) rings which are floppy, where the methyl groups can move

(23) Kress, J. D. Unpublished work.

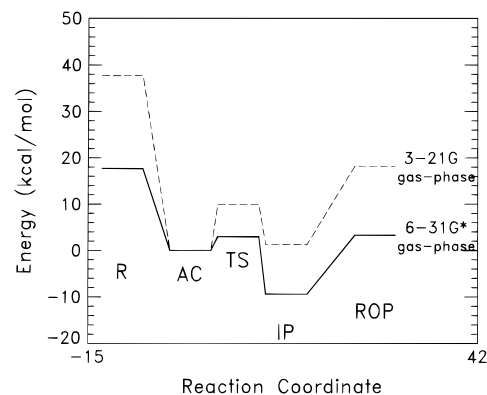


**Figure 3.** The gas-phase reaction path of KOH catalyzed ring-opening polymerization of D<sub>3</sub> calculated with the HF method: 3-21G (dashed line); 6-31G\* (solid line). As specified, either 3-21G or 6-31G\* basis sets are used for Si and O for both the energy and geometry calculations. The LANL2DZ ECP basis set is used for K and the STO-3G basis set is used for the CH<sub>3</sub> groups. The structures along the reaction coordinate are defined in Figure 1. The addition complex (AC) is defined as the zero of energy for both cases. The reaction coordinate is not to scale and is only representative.

away from the center of the ring. Further unconstrained geometry optimization with the 3-21G basis revealed that both the side-on and multidentate adducts are metastable with respect to an addition complex discussed next.

When the constrained side-on or multidentate adduct is allowed to fully relax, atom O(32) in the KOH molecule forms a bond with atom Si(3) and the atom K(31) forms bonds with ring atom O(1) and KOH atom O(32). This is shown in Figure 1 (structure AC). The atom Si(3) is 5-fold coordinated with atom O(32) (KOH) and a ring atom O(5) in the axial positions and the two methyl groups and another ring atom [O(1)] in the equatorial positions. The KOH molecule is nearly in the plane of the ring, although the ring itself is not perfectly planar.

To this point the reaction path from the reactants to the addition complex has been downhill. To continue, a reaction coordinate *r* is defined to be the Si–O bond stretch involving the 5-coordinated atom Si(3) and atom O(1) in the ring of the addition complex. The reaction coordinate was determined manually in increments of typically  $\Delta r = 0.2$  Å starting at the addition complex geometry (defined as *r* = 0). The Si(3)–O(1) distance in the AC is 1.75 (3-21G) and 1.74 Å (6-31G\*).

**Table 3.** Critical Points Along the Gas-Phase Reaction Path for KOH Catalyzed Ring-Opening Polymerization of D<sub>3</sub>

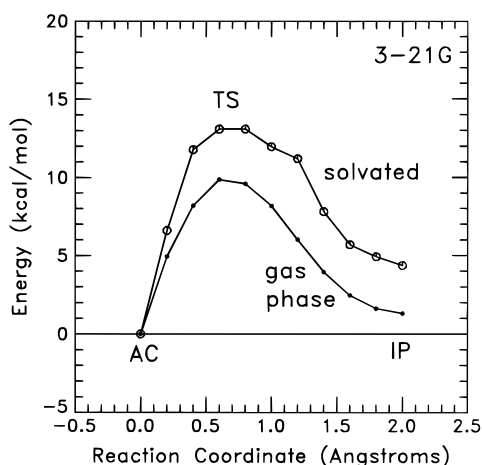
	basis set <sup>a</sup> geometry <sup>b</sup> method <sup>c</sup>	electronic energy (kcal/mol)				
		3-21G	6-31G*	6-31G*	"AE"	6-31G*
		3-21G HF	3-21G HF	6-31G* HF	"AE" HF	6-31G* MP2
reactants (R)		38	18	18	15	27
addition Complex (AC)		0	0	0	0	0
barrier (TS)		10	3	3	<i>d</i>	2
insertion product (IP)		1	-12	-9	<i>d</i>	-5
ring-opened product <sup>e</sup> (ROP)		18	7	3	<i>d</i>	11

<sup>a</sup> Basis set used for Si and O to evaluate the energy. (For K the LANL2DZ ECP was used. For C and H, the STO-3G basis set was used.) For the case labeled "AE", the all electron basis<sup>25</sup> was used for K, 6-31G\* for Si, 6-31+G\* for O, and 3-21G for C and H. <sup>b</sup> Basis set used to optimize the geometry. The Hartree-Fock (HF) method was used for all optimizations. <sup>c</sup> Method used to evaluate energy for a given optimized geometry. MP2 is second order Møller-Plesset perturbation theory. <sup>d</sup> Not calculated. <sup>e</sup> Ring-opened product energy computed with the "fixed *r*" approach. (See text for explanation.)

**Table 4.** Critical Points Along the Solvated (in THF) Reaction Path for KOH Catalyzed Ring-Opening Polymerization of D<sub>3</sub>

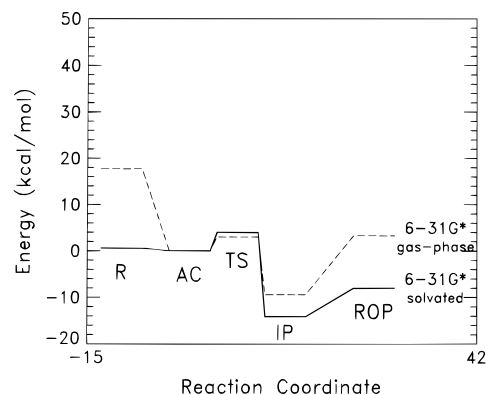
	Si,O basis set <sup>a</sup> geometry <sup>b</sup> method <sup>c</sup>	potential of mean force, <i>W</i> (kcal/mol)		
		3-21G	6-31G*	6-31G*
		3-21G HF	6-31G* HF	6-31G* MP2 <sup>d</sup>
reactants		25	1	10
addition complex		0	0	0
barrier		13	4	3
insertion product		4	-14	-10
ring-opened product <sup>e</sup>		10	-8	0

<sup>a</sup> Basis set used to evaluate the energy. In all cases, for K, the LANL2DZ ECP was used, and, for C and H, the STO-3G basis set was used. <sup>b</sup> Basis set used to optimize the geometry. The Hartree-Fock (HF) method was used for all optimizations. <sup>c</sup> Method used to evaluate energy for a given optimized geometry. MP2 is second order Møller-Plesset perturbation theory. <sup>d</sup> The potential of mean force was computed by adding  $\Delta G(\text{sol})$  for the HF/6-31G\* case to the MP2/6-31G\* gas-phase electronic energy. <sup>e</sup> Ring-opened product energy computed with the "fixed *r*" approach. (See text for explanation.)



**Figure 4.** The potential of mean force (open circles) and gas-phase electronic energy (dots) for the reaction path of KOH catalyzed ring-opening polymerization of D<sub>3</sub> (3-21G basis for Si and O for both the energy and geometry calculations). The reaction coordinate is shown from the addition complex (*r* = 0) to the insertion product. (The structures are defined in Figure 1.) The zero of energy for each curve is the addition complex.

Every coordinate was optimized in the system except the reaction coordinate. The initial geometry in the optimization was taken from the result of the previous step. A barrier (transition state, TS) of 10 kcal/mol is found at *r* = 0.6 Å for the 3-21G basis, whereas the larger 6-31G\* basis gives a lower barrier of 3 kcal/mol at *r* = 0.2 Å. The Si(3)-O(1) distance in the TS is 2.35 (3-21G) and 1.94 Å (6-31G\*).

(24) Schlegel, H. B. *J. Comput. Chem.* **1982**, 3, 214.

**Figure 5.** The reaction path of KOH catalyzed ring-opening polymerization of D<sub>3</sub> calculated with the HF method: gas-phase (dashed line); potential of mean force, solvated (solid line). 6-31G\* basis sets are used for Si and O for both the energy and geometry calculations. A STO-3G basis set is used for the CH<sub>3</sub> groups and the LANL2DZ ECP is used for K. The structures along the reaction coordinate are defined in Figure 1. The addition complex (AC) is defined as the zero of energy for both cases. The reaction coordinate is not to scale and is only representative.

The manually-optimized structure was refined using the gradient optimization procedure<sup>24</sup> in GAUSSIAN 94. This procedure is most efficient at finding transition states when the full Hessian (second derivative) matrix is computed for at least the first optimization step. Second derivatives using effective core potentials (ECPs) are currently<sup>13</sup> computed numerically in GAUSSIAN 94, resulting in an order of magnitude greater CPU time compared to analytic second derivatives using an all-electron (AE) basis. Therefore an AE basis set<sup>25</sup> was used for the K atom, consisting of six contracted s-type functions and three contracted p-type functions, and augmented with two more diffuse p-type functions (exponents of 0.0376 and 0.014). These diffuse functions render the AE and LANL2DZ basis sets of comparable quality. For example, using the 6-31G\* basis for Si and O and the STO-3G basis for C and H, the energy of the reactants relative to the addition complex using the AE and ECP for the K atom is 21 and 18 kcal/mol, respectively.

A transition state search was started from the manually-optimized ECP/3-21G geometry, *r* = 0.6 Å, in the AE/3-21G basis. A proper transition state (one negative force constant) was found at *r* = 0.67 Å for the AE/3-21G basis, with an energy of 12 kcal/mol relative to the addition complex. When the same procedure was tried in the AE/6-31G\* basis starting from the ECP/6-31G\* geometry, no negative force constant was found and hence the gradient search process could not proceed.

Various attempts were also made using Quadratic Synchronous Transit<sup>26</sup> (QST) techniques to find the transition state in

(25) Schafer, A.; Huber, C.; Ahlrichs, R. *J. Chem. Phys.* **1994**, 100, 5829.

the AE/6-31G\* with only partial success. A QST optimization with GAUSSIAN 94 was attempted using the AC, IP, and manually-optimized TS structures (ECP/6-31G\*) as the three required input structures (reactants, products, and intermediate). This calculation failed to find a proper transition state. The QST optimization was repeated with the AC, IP, and manually-optimized TS structures (AE/6-31G\*) and failed as well. Since the manually-optimized ECP/3-21G TS structure has a larger  $r$  than the ECP/6-31G\* TS structure, the ECP/3-21G structure was optimized using the AE/6-31G\* basis holding  $r = 0.6$  Å fixed. This gives a barrier of 3.7 kcal/mol relative to the AC structure and one negative force constant. This constrained structure was then used as the starting point for the optimal AE/6-31G\* value for  $r$  with the full Hessian computed at each step. At  $r = 0.5$  Å the optimization algorithm aborted due to a lack of a negative force constant, with a barrier energy of 4.5 kcal/mol relative to the AC structure. We conjecture that the potential energy hypersurface has a complicated, but subtle, topography, and is very flat (3 to 5 kcal/mol relative to the AC) around the manually-optimized "transition state" region. Therefore, no further attempts were made to find a proper 6-31G\* transition state.

The nature of 5-coordinate Si species, either as stable forms or reactive intermediates, has been the subject of numerous recent experimental and theoretical studies.<sup>27–29</sup> X-ray crystal structures have been reported for a variety of 5-coordinate Si compounds, of which the closest forms to the present siloxane systems include the bicyclics  $\text{Si}(\text{O}-\text{C}_2-\text{O})_2\text{R}^-$  and  $\text{Si}(\text{O}-\text{C}_2-\text{O})_2\text{X}^-$ , where R and X denote alkyl and halide ligands, respectively, and  $\text{C}_2$  denotes intervening aliphatic or aromatic carbon linkages in the bidentate rings. A few anionic structures with pentaoxy ligands  $\text{Si}(\text{O}-\text{C}_2-\text{O})_2(\text{OR})^-$  have also been reported. The 5-coordinate species we observe in the present calculations would be of the form  $\text{Si}(\text{OR})_3(\text{CH}_3)_2^-$  where, as shown in AC in Figure 1, atoms O(5) and O(32) form the apices and atom O(1) forms one equatorial position of a trigonal bipyramid (TBP); the two methyl groups C(16) and C(17) form the other two equatorial positions. The calculated 6-31G\* angles for this structure are as follows (Table 2):  $\text{O}_{\text{ax}}-\text{Si}-\text{O}_{\text{ax}}$  ( $174.15^\circ$ ),  $\text{O}_{\text{ax}}-\text{Si}-\text{O}_{\text{eq}}$  ( $91.10^\circ$  and  $83.05^\circ$ ), and  $\text{C}_{\text{eq}}-\text{Si}-\text{O}_{\text{eq}}$  ( $118.77^\circ$  and  $118.91^\circ$ ), where  $\text{ax} = \text{axial}$  and  $\text{eq} = \text{equatorial}$ . Going from the addition complex to the transition state (Figure 1 and Table 2), the equatorial atom O(5) becomes axial and the two axial atoms [O(5) and O(32)] become equatorial. Also, one of the equatorial methyl groups C(15) becomes axial. We speculate that our difficulty in finding a proper transition state using the 6-31G\* basis is due to the fact that the transition state optimization algorithms could not follow the complex coupling between the reaction coordinate (Si–O bond stretch) and the pseudorotation (two axial O atoms on the 5-coordinate Si atom rotating in the AC to a methyl group and the reaction coordinate in the axial positions in the TS). Experimental structures for 5-coordinate Si compounds span the range along the coordinate between TBP and the rectangular pyramid (RP). As R becomes progressively less bulky for the pentaoxy  $\text{Si}(\text{O}-\text{C}_2-\text{O})_2(\text{OR})^-$  series,<sup>29</sup> the structures change from TBP to RP, while the  $\text{Si}(\text{O}-\text{C}_2-\text{O})_2\text{X}^-$  species tend more toward TBP. Other penta-coordinate structures have been invoked in sol-gel synthesis<sup>30</sup> and zeolite formation<sup>31</sup> from silica-containing precursors. Re-

cent evidence has also been reported on 5-coordinate cationic structures in acid-catalyzed siloxane polymerization,<sup>32</sup> as contrasted to anionic forms we find here in base-catalyzed siloxane polymerization.

The mechanism in Figure 1 corresponds to the situation where the incoming  $\text{OH}^-$  group associated with  $\text{K}^+$  occupies an axial position of the TBP and the leaving O–Si group of the  $\text{D}_3$  ring occupies an equatorial position. In this situation, retention of stereochemistry about the Si is maintained in the formation and cleavage of the Si–O bonds, as has been discussed earlier.<sup>27–29</sup> Inversion stereochemistry results in the standard  $\text{S}_{\text{N}}2$  chemistry involved in C chemistry, where both entering and leaving groups occupy the axial positions of the TBP transition state. In the present case of OH attack on siloxane, the TBP form is a stable point along the reaction coordinate.

The next step on the reaction path in Figure 3, the minimum at  $r = 2.0$  Å, corresponds to the insertion of KOH into the  $\text{D}_3$  ring, where atom K(31) is inserted between the Si(2)–O(1) and O(32)–H(33) groups. This is designated as a insertion product (Figure 1, structure IP).

The final point in Figure 3 corresponds to the ring-opened product (Figure 1, structure ROP). Because optimizing a floppy molecule which has many local minima is difficult, if not impossible, this energy was calculated two different ways. The first approach fixed  $r$  and optimized all other coordinates. This yields a nearly "linear" ring-opened product for  $r = 6.75$  Å, with a 3-21G energy of about 18 kcal/mol relative to the addition complex. The second approach constrained  $\text{a}(\text{Si}-\text{O}-\text{Si})$  to  $180^\circ$  and optimized all other coordinates (except for a few dihedral angles). This structure is the ideal "linear" ring-opened product and has a 3-21G energy of 24 kcal/mol relative to the addition complex. The fixed  $r$  approach is more stable than the constrained approach by about 4–5 kcal/mol. This is probably because it allows the OK and OH termini to interact, whereas the constrained approach does not. A ring-opened product energy of 3 kcal/mol relative to the addition complex was calculated with the 6-31G\* basis using the first approach with  $r = 5.64$  Å fixed.

The present results suggest that the insertion product is more stable than the ring-opened product. However, this energy difference can be an artifact of limitations in the gas-phase models. The K cation in the ring-opened product can be considered coordination unsaturated. In solution, the K atom can interact and coordinate with Si–O moieties in unreacted  $\text{D}_3$  and PDMS in the environment.

Force constant matrix calculations were performed to classify various points along the reaction path. All positive force constants, and thus, proper local minima, were found for the reactants, addition complex, and insertion product using the AE/6-31G\* basis. A single negative force constant was found for the ECP/3-21G and AE/3-21G TS structures, thus verifying that both are proper transition states. As discussed earlier, proper ECP/6-31G\* and AE/6-31G\* transition states were not found.

The general trend of the variation of geometries and atom charges along the reaction path [the Si(3)–O(1) bond] is summarized in Table 2. The change in bond angles between AC and TS was discussed above in terms of a trigonal bipyramidal structure about the 5-fold coordinated atom Si(3). The bond between Si(3) and the KOH O atom [Si(3)–O(32)] shrinks by about 0.2 Å between the AC and TS. The distance [K(31)–O(32)] between the K and O atoms from KOH gradually increases as the reaction path is traversed from R to IP. For the reaction path bond [Si(3)–O(1)] there is less charge

(26) Halgren, T. A.; Lipscomb, W. N. *Chem. Phys. Lett.* **1977**, *49*, 225. Peng, C.; Schlegel, H. B. *Isr. J. Chem.* **1994**, *33*, 449.

(27) Holmes, R. R. *Chem. Rev.* **1990**, *90*, 17.

(28) Corriu, R. J. P.; Young, J. C. In *The Chemistry of Organic Silicon Compounds*; Patai, S., Rappoport, Z., Eds.; John Wiley and Sons: Chichester, 1989; pp 1241–1288.

(29) Holmes, R. R.; Day, R. O.; Payne, J. S. *Phosphorus, Sulfur, Silicon* **1989**, *42*, 1.

(30) Iler, R. K. *The Chemistry of Silica*; Wiley: New York, 1979.

(31) Herreros, B.; Carr, S. W.; Klinowski, J. *Science* **1994**, *263*, 1585. Herreros, B.; Klinowski, J. *J. Phys. Chem.* **1994**, *99*, 1025.

(32) Olah, G. A.; Li, X.-Y.; Wang, Q.; Rasul, G.; Surya Prakash, G. K. *J. Am. Chem. Soc.* **1995**, *117*, 8962.

(CHELPG) separation for the AC compared to both R and TS. The charge on atom O(32) from KOH increases in increments of about 0.2 going from R to AC to TS. However, the change in the K(31) atom charge along the reaction path is negligible.

A summary of the effect of basis set and electron correlation along the KOH–D<sub>3</sub> gas-phase reaction path is given<sup>33</sup> in Table 3. (The manually-optimized 6-31G\* “transition state” structure is reported in Table 3.) Relative to the addition complex energy, electron correlation (MP2 calculations) increases the reactants energy and decreases the barrier to products. The better basis (6-31G\*) has a more dramatic effect relative to the 3-21G energies; the reactants energy is reduced from 38 to 18 kcal/mol and the difference between the barrier energies is reduced from 10 to 3 kcal/mol relative to the 3-21G values. An even larger basis set (denoted AE in Table 3) yields a much smaller change in the reactants energy relative to the 6-31G\* value (18 vs 15 kcal/mol, respectively). Note that single point energy calculations with the 6-31G\* basis using the 3-21G optimized structures compare reasonably well with the 6-31G\* energies calculated with the 6-31G\* optimized geometries. Since geometry optimization along the reaction path is the most computationally demanding step, the strategy of optimizing with a smaller basis set followed by a single point calculation with a larger basis set will allow affordable calculations on larger siloxane molecules considered in future work.<sup>23</sup>

The effect of basis set superposition errors<sup>34</sup> (BSSE) on the relative energies between R (the KOH and D<sub>3</sub> reactants) and AC (the addition complex) was examined for various basis sets. An upper bound for this effect is obtained by computing the sum of (1) the energy difference for KOH in the AC geometry with and without the presence of the D<sub>3</sub> basis functions and (2) the D<sub>3</sub> moiety in the AC geometry with and without the KOH basis functions. For the [6-31G\*(Si,O)/STO-3G(C,H)/LANL2DZ-(K)] basis set, which is reasonably accurate for the Si–O portions of the molecule, the BSSE estimate is reasonably large (14 kcal/mol) and of the same size as the reaction energy for KOH addition (18 kcal/mol). For the more flexible [6-31G\*(Si)/6-31+G\*(O)/3-21G(C,H)/AE(K)] basis, the BSSE estimate is considerably smaller (5 kcal/mol) as compared to the R–AC difference of 15 kcal/mol. It is less clear, however, in such cases where strong covalent bonds are being formed, whether BSSE estimates are meaningful corrections to computed thermochemistries. Typically such estimates are used in weakly-bound complexes, such as hydrogen-bonded species, where the two moieties retain their molecular identity.

**Solvation Calculations.** The shape of the potential of mean force in the solvent (Figure 4) is similar to the gas-phase potential energy curve, although there is a shoulder evident in the potential of mean force which is not present in the gas-phase energy. Both curves exhibit a barrier between the stable addition complex and the insertion product. The solvated barrier height has increased to 13 kcal/mol from the 3-21G gas-phase value of 10 kcal/mol. For 3-21G, the solvated curve is roughly 3 kcal/mol higher than the gas-phase curve from the AC to IP. The 3-21G solvated ROP relative to the AC is 8 kcal/mol lower than the gas-phase value (Table 3 vs Table 4). In general, the IP and ROP are stabilized more by the solvent, relative to the AC and TS, since the IP and ROP structures are more open.

(33) The reactants (D<sub>3</sub>) structures and energies reported in Tables 2, 3, and 4 and in Figures 1 and 3 were optimized with constraints on the  $d(\text{C}-\text{Si}-\text{O}-\text{O}) = 120^\circ$  and  $d(\text{H}-\text{C}-\text{Si}-\text{C}) = 60^\circ$  dihedral angles. When the structures were further optimized by relaxing the constraints, the 3-21G and 6-31G\* energies were lowered by 2 and 1 kcal/mol, respectively. The fully-optimized coordinates are reported in Table 1.

(34) Frisch, M. J.; Del Bene, J. E.; Binkley, J. S.; Schaefer, H. F., III *J. Chem. Phys.* **1986**, *84*, 2279.

The openness exposes the Si and O atoms in the ring more to the solvent and, thus,  $\Delta G(\text{sol})$  is more negative.

For the HF/6-31G\* solvated calculations (Figure 3 and Table 4), the transition state energy is equal to the reactants energy; the ring-opened product energy is 9 kcal/mol below the reactants energy; and the barrier energy relative to the addition complex is 4 kcal/mol. The general effect of the 6-31G\* relative to the 3-21G basis set along the solvated reaction path is to stabilize (lower) the potential of mean force relative to the AC energy. To provide a quantitative estimate of the solvated reaction path including electron correlation, MP2 potentials of mean force (Table 4) were generated by adding  $\Delta G(\text{sol})$  calculated with a HF/6-31G\* wave function (first column, Table 4) to the MP2/6-31G\* gas-phase electronic energy.

## Conclusion

*Ab initio* electronic calculations were conducted to examine a reaction path for the KOH catalyzed ring-opening polymerization of hexamethylcyclotrisiloxane (D<sub>3</sub>). The overall picture that emerges is initial side-on attack by KOH on a Si–O bond in the D<sub>3</sub> ring (Figure 1, structure R) leading to a stable addition complex (Figure 1, structure AC) with a 5-fold coordinated Si atom. The reaction path leads to a five-coordinate transition state (Figure 1, structure TS), then to a stable insertion product (Figure 1, structure IP). The stability of a ring-opened product (Figure 1, structure ROP) is also considered. The transition state (and stable addition complex) contains a 5-fold coordinated Si atom and is not a multidentate (“crown-ether”) structure. The energy along the reaction path was modeled both in the gas phase and in a moderately polar solvent (tetrahydrofuran, THF). The solvation energy was calculated using a recent implementation<sup>22</sup> of an electrostatic model, where the solute molecule is placed in a non-spherical cavity in a dielectric continuum. The effect of basis set and electron correlation on the gas-phase energy and the effect of basis set on the solvation energy were studied. Along the solvated reaction path calculated at the Hartree–Fock level (with a 6-31G\* basis set for the Si and O atoms), the apparent transition state energy is nearly equal to the reactants energy and is 4 kcal/mol above the addition complex energy. The effect of electronic correlation (Moller–Plesset 2nd-order perturbation theory) on the 6-31G\* gas-phase reaction path destabilizes (increases) the reactants and ring-opened product energies relative to the addition complex; however, the transition state relative energy change is negligible.

Finally, we note that the solvation model does not include the direct interaction of the electronic structure of a solvent molecule with the solute. For example, an O atom on a THF molecule could participate in multidentate bonding with the K atom and an O atom in the D<sub>3</sub> ring. Such solvation models that involve a few solvent molecules explicitly coupled with a dielectric continuum description may be an avenue for future work.

**Acknowledgment.** We thank Stefan Klemm, Smarajit Mitra, David Misemer, Richard Martin, Lawrence Pratt, John Blair, Shih-Hung Chou, and Kris Zaklika for many valuable discussions and Holman Brand for assistance with the graphics. This work was supported by a Cooperative Research and Development Agreement (CRADA) “Properties of Polymers and Organic Dye Molecules” between the 3M Corporation and Regents of the University of California/Los Alamos National Laboratory (LANL). The work at LANL is carried out under the auspices of the U.S. Department of Energy, Contract No. W-740-ENG-36.